Intelligent PD Control of a Coaxial Birotor UAV for Precise Trajectory Tracking Using Metaheuristic Algorithms

Mohamed AZEGMOUT[1]*, Mostafa MJAHED[2], Abdeljalil EL KARI[1], Hassan AYAD[1]

[1] Laboratory for Electrical Systems, Energy Efficiency, and Telecommunications (LSEEET), The Faculty of Sciences and Techniques (FSTG) of Marrakech, Cadi Ayyad University, Abdelkrim El Khattabi Blvd., B.P. 618, Marrakesh, 40000, Morocco
mohamed.azegmout@gmail.com (*Corresponding author*), a.elkari@uca.ma, h.ayad@uca.ma

[2] Mathematics and Systems Department, Royal School of Aeronautics, Marrakesh, 40000, Morocco
mjahed.mostafa@gmail.com

Abstract: This paper presents the design and optimization of a Proportional-Derivative (PD) control scheme for tracking the trajectory of a coaxial birotor unmanned aerial vehicle (UAV). The mathematical model for this UAV was derived by using the Newton–Euler formalism, which captures the nonlinear and coupled dynamics of its six degrees of freedom. Six independent PD controllers were designed for regulating the translational motions (x,y,z) and the rotational motions (ϕ, θ, ψ). In order to overcome the limitations of classical tuning, four meta-heuristic algorithms (the Invasive Weed Optimization (IWO) algorithm, Ant Colony Optimization (ACO) algorithm, Cultural Algorithm (CA) and Black Hole Algorithm (BHA)) were employed for optimally tuning the PD controller gains. Further on, the proposed control strategy was validated for two trajectory tracking scenarios which represent typical UAV navigation tasks. Additionally, robustness tests were conducted under external disturbances for evaluating the stability and disturbance rejection performance of the coaxial birotor UAV. Also, comparative simulations were carried out for assessing the tracking error (mean squared error), overshoot, and settling time for the analysed UAV, demonstrating that meta-heuristic-based tuning considerably improved the accuracy, robustness, and dynamic response in comparison with the conventional methods. The obtained results highlight the effectiveness of intelligent optimization for enhancing UAV control, particularly for a precise and stable trajectory.

Keywords: UAV, Coaxial Birotor, ACO, CA, IWO, BHA, Nonlinear control system, Trajectory Tracking, PID/PD.

1. Introduction

Unmanned Aerial Vehicles (UAVs) have become a central focus of research and development due to their wide range of applications in surveillance, environmental monitoring, infrastructure inspection, and autonomous delivery. Among various UAV configurations, Vertical Take-Off and Landing (VTOL) systems offer the advantage of hovering and precise maneuvering in constrained environments (Rakha & Gorodetsky, 2018).

In the traditional quadrotor design, two pairs of counter-rotating propellers are attached to a center body in a plus or cross arrangement. Quadrotors have an excellent maneuverability in controlled roll and pitch motions and a strong stability in hovering due to their mechanical simplicity. However, because quadrotors have four propellers, their thrust efficiency or highest thrust per platform area, is typically constrained.

One of the key indicators of UAV performance is the thrust-to-platform area ratio, which directly affects flight endurance and energy efficiency (Driessens & Pounds, 2015). In recent years, several coaxial UAV configurations have been developed to enhance stability and maneuverability (Koehl et al., 2012; Niu et al., 2015; Wang et al., 2017). To accurately describe their dynamics, researchers have employed both the Newton–Euler (Darvishpoor et al., 2015; Roussel et al., 2016) and Euler–Lagrange (Donadel et al., 2014) modeling frameworks.

In electromechanical systems, proportional integral derivative (PID) control is arguably the most often utilized technique for attaining tracking or regulation. Unmanned aerial vehicles represent a common application of this technique. Numerous recent studies have documented the benefits of utilizing a PID controller. Alaimo et al. (2014) applied a PID controller to a hexacopter UAV, demonstrating an effective stabilization and trajectory tracking. Their results showed an improved attitude and altitude control with an enhanced robustness against disturbances and model uncertainties. For instance, in (Pounds, 2012), the stability of a PID controller used on a helicopter was examined for the tasks of hovering and balanced flying with the addition of a payload mass. The primary difficulty with PID controllers is accurate and efficient parameter adjustment. In practice, PID parameter tuning is challenging because controlled systems frequently experience time delay and nonlinearity.

https://doi.org/10.24846/v35i2y202602

Recent studies have introduced various nonlinear control strategies for UAV motion control. Xu et al. (2021) used a backstepping sliding mode controller for birotor stabilization, while Xu et al. (2022) applied dynamic feedback linearization for coaxial UAV tracking. Nkouagnou et al. (2021) proposed a generalized predictive control with a PI-observer to achieve a precise birotor trajectory tracking. For quadrotor UAVs, Ezzara et al. (2025) proposed an adaptive backstepping active fault-tolerant control approach that estimates actuator faults and disturbances using a nonlinear adaptive observer.

During the last two decades, various artificial intelligence (AI) techniques such as neural networks, fuzzy systems, and neuro-fuzzy techniques have been widely employed for PID tuning to obtain optimal controller parameters (El Hamidi et al., 2022; Mjahed, 2019; Qin, 2025). Due to their great effectiveness in identifying the optimal solution within a problem area, certain meta-heuristic techniques have also garnered a lot of attention lately. Some of these algorithms that have been suggested in the literature have also been used in UAV control. For instance, in (Portillo et al., 2023), three distinct control strategies (classical PID, Super Twisting, and Adaptive Sliding Mode) are adjusted using the PSO (Particle Swarm Optimization) algorithm and contrasted for the translation control for an unmanned aerial vehicle with a single rotor (SR-UAV). In (El Gmili et al., 2019a) a PSO-based approach was developed for tuning the PD parameters for a tilt-rotor UAV flight control and trajectory tracking, with results showing that the system maintained stability and accurately followed the desired trajectories even under external disturbances. For quadrotor trajectory tracking in (Siti et al., 2019), two methods of control are suggested, namely the Reference Model (RM) method and Genetic Algorithm (GA) optimization, and the authors compare the performance of PD and PID controllers and evaluate robustness under environmental disturbances.

Other algorithms, such as Differential Evolution (DE), Ant Lion Optimizer (ALO), Bat Algorithm (BA) and Harmony Search (HS) Algorithm were also used for PID tuning for different systems` behavior (Fayti et al., 2023). In (Ait Dahmad et al., 2025) the multivariate Gaussian mixture model-ant colony optimization (MGMM-ACO) approach that enhances the conventional ACO by modeling intervariable dependencies, is used for tuning an adaptive MPC controller.

The coaxial birotor UAV represents a compact and mechanically efficient alternative to traditional rotorcraft designs. Its coaxial arrangement, consisting of two counter-rotating rotors mounted on the same vertical axis, inherently cancels out the reactive torque generated by each rotor. This eliminates the requirement for a tail rotor, resulting in a symmetric and space-efficient configuration. In addition to its structural advantages, the coaxial design enhances yaw stability and lift efficiency, which makes it particularly well-suited for missions in indoor or constrained environments. Despite these mechanical benefits, the dynamic behavior of coaxial birotor UAVs remains nonlinear and highly coupled, creating substantial challenges in both modeling and control. Consequently, the accurate representation of the vehicle's translational and rotational dynamics is essential for ensuring an effective control and a reliable flight performance.

In this study, a comprehensive mathematical model of the employed vehicle is formulated based on the Newton–Euler formalism, capturing both the translational motion and the rotational dynamics of the platform. To address the control challenge, a multi-loop control scheme is proposed, comprising six PD controllers dedicated to regulating the UAV's attitude (roll (ϕ), pitch (θ), and yaw (ψ)) and position (x, y, and z). While PID controllers are known for their simplicity and real-time applicability, their performance heavily depends on the precise tuning of control gains. Therefore, four meta-heuristic optimization techniques (CA, BHA, ACO and IWO) are employed to determine the optimal parameters of each controller, enhancing stability, response time, and robustness against disturbances and model uncertainties. No single method can provide the optimal solution for all optimization problems, as each algorithm performs differently depending on the specific task. Therefore, it is essential to evaluate the suitability of each method for a given problem.

The scientific contributions of this paper are summarized as follows:

- A systematic and fair comparison of four meta-heuristic optimization methods (ACO, CA, IWO and BHA) used for adjusting a birotor coaxial UAV's proportional-derivative (PD) controller settings;

- All algorithms are implemented under identical experimental conditions, including the same objective function, parameter bounds, population size, and maximum number of iterations, ensuring reproducibility and fairness;

- Four statistical indicators (the best, worst, average, and standard deviation of the objective function values) are used in order to objectively evaluate each algorithm's performance over the course of five separate runs.

The remainder of this paper is structured as follows. The coaxial birotor dynamical model is described in Section 2, while Section 3 presents the four selected meta-heuristic algorithms. Section 4 describes the proposed control design methodology, including the ACO, CA, IWO and BHA approaches. Further on, Section 5 presents and discusses the findings of the simulations and experiments which were carried out. Finally, Section 6 provides the conclusion of this paper, while outlining possible future research directions.

2. Dynamic Modelling of Birotor Coaxial UAV

As illustrated in Figure 1, the coaxial birotor UAV is a compact VTOL platform engineered to provide a superior maneuverability and adaptability in restricted environments. Its configuration incorporates two counter-rotating rotors mounted on a common vertical axis, in contrast to traditional helicopters (Bermes, 2010; Nonami et al., 2010), this design eliminates the need for a swashplate to modulate blade pitch. Instead, it utilizes a fixed-pitch rotor system, where control is primarily achieved by adjusting rotor speeds in combination with two auxiliary servomotors.

The dynamic modeling of the Birotor Coaxial UAV is carried out by using the Newton–Euler formalism, which provides a systematic framework to obtain the translational and rotational movement equations for rigid bodies. The model captures all six degrees of freedom (6-DOF) of the UAV, including linear motion (x, y, z) and angular motion (roll (ϕ), pitch (θ), and yaw (ψ)). An inertial frame $O_E(X_E, Y_E, Z_E)$ and a body-fixed frame $O_B(X_B, Y_B, Z_B)$ attached to the birotor coaxial UAV are considered. The UAV's position in space is defined by the translational coordinates (x, y, z), while its orientation is expressed through the Euler angles (ϕ, θ, ψ), representing the roll, pitch, and yaw, respectively.

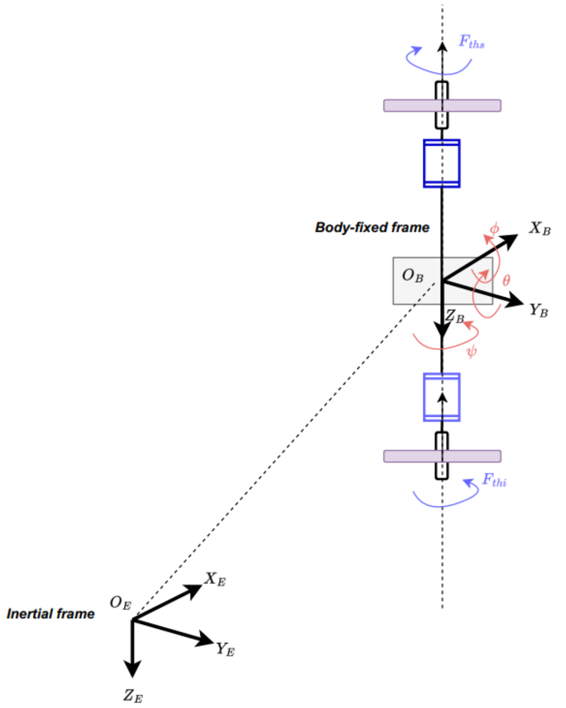

Figure 1. Birotor Coaxial Configuration

The modeling of the birotor coaxial UAV follows the work of Mjahed & Said (2018), the same model was validated through the identification of different outputs by using Cultural Algorithms (Azegmout et al., 2024).

$$\ddot{x} = \frac{1}{m}\left[\frac{1}{2}\rho S C_{yx} 0.1(1+\alpha) R^2 \left(\Omega_{hi}^2 + \Omega_{hs}^2\right) - \left(C_s + C_i + C_{cx}\right)\dot{x}^2\right] \quad (1)$$

$$\ddot{y} = \frac{1}{m}\left[\frac{1}{2}\rho S C_{yy} 0.1(1+\beta) R^2 \left(\Omega_{hi}^2 + \Omega_{hs}^2\right) - \left(C_s + C_i + C_{cx}\right)\dot{y}^2\right] \quad (2)$$

$$\ddot{z} = \frac{1}{m}\left[-mg + \left(b_s + b_i\right)\left(\Omega_{hi}^2 + \Omega_{hs}^2\right)\right] \quad (3)$$

$$\ddot{\phi} = \frac{L_d}{2I_x}\left[\begin{array}{l} b_s\left(\cos(\phi)\sin(\theta)\cos(\psi) + \sin(\phi)\sin(\psi)\right) \\ \left(\Omega_{hi}^2 + \Omega_{hs}^2\right) - \left(C_s + C_i + C_{cy}\right)\dot{y}^2 \end{array}\right] \quad (4)$$

$$\ddot{\theta} = \frac{L_d}{2I_y}\left[\begin{array}{l} b_s\left(\cos(\phi)\sin(\theta)\sin(\psi) - \sin(\phi)\cos(\psi)\right) \\ \left(\Omega_{hi}^2 + \Omega_{hs}^2\right) - \left(C_s + C_i + C_{cx}\right)\dot{x}^2 \end{array}\right] \quad (5)$$

$$\ddot{\psi} = \frac{L_d}{2I_z}\left[d_{hs}\left(\Omega_{hi}^2 - \Omega_{hs}^2\right)\right] \quad (6)$$

with $b_s = b_i = \frac{1}{2}\rho S C_T$,

where S is the surface obtained by the rotation of the propellers and C_T is the propeller's thrust coefficient, while Ω_{hs} and Ω_{hi} are the propellers' angular velocities, expressed in (rad/s). The first lateral lift coefficient, represented by C_{yx}, is equal to 0.1 (1+α), while the second lateral lift coefficient, represented by C_{yy}, is equal to 0.1

(1+β). C_{cy} and C_{cx} are drag constants related to the helicopter body, and C_i and C_s are drag coefficients related to the propellers.

3. Meta-heuristic Algorithms Used

3.1 Ant Colony Optimization (ACO)

Numerous difficult combinatorial optimization problems have been solved by using the graph-based meta-heuristic method known as the ACO Algorithm. The fundamental idea of ACO was first formulated by Marco Dorigo (Dorigo, 1992). The search for the least expensive route across a graph should be carried out to illustrate the problem under discussion. This network is searched for helpful paths by artificial ants. Ants usually only locate roadways of a rather poor quality on their own due to their extremely basic behavior, better paths are found as a result of the colony ants' worldwide cooperation.

According to local pheromone updating criteria, each ant in the proposed technique modifies the pheromone levels on the trails it traveled after a tour.

$$\tau(k)_{ij} = \tau(k-1)_{ij} + \frac{0.01\theta}{f} \tag{7}$$

The difference in pheromone values between *(i)* and *(j)* is denoted by $\tau(k)_{ij}$ at iteration *k*, where θ is the overall refresh coefficient for pheromones and the objective function related to the cost of the ants` tour is denoted by *f*.

Equations (8) and (9) alter the pheromone routes of the best and worst ant colony tours in accordance with the global pheromone updating rule:

$$\tau(k)_{ij}^{best} = \tau(k)_{ij}^{best} + \frac{\theta}{f_{best}} \tag{8}$$

$$\tau(k)_{ij}^{worst} = \tau(k)_{ij}^{worst} - \frac{0.3\theta}{f_{worst}} \tag{9}$$

The symbols "τbest" and "τworst", respectively, represent the pheromone levels for the ant routes with the f_{best} and f_{worst} costs.

There are much more pheromones on the best tour of the ant colony's trails than on the worst tour. Pheromone evaporation enables the ACO algorithm to 'forget' previous paths, allowing it to concentrate its search more effectively and prevent it from getting stuck in local minima. For expressing concentrations, the evaporation constant λ is used in equation (10) (Varol & Bingul, 2004):

$$\tau(k)_{ij} = \tau(k)_{ij}^{\lambda} + \left(\tau(k)_{ij}^{best} + \tau(k)_{ij}^{worst}\right) \tag{10}$$

Ünal et al. (2013) provides a detailed description of the main steps of the ACO algorithm used.

3.2 Cultural Algorithm (CA)

Robert Reynolds (Reynolds, 1994) introduced the concept of cultural algorithm, which is a method of evolutionary computing that draws inspiration from the process of cultural evolution related to human cultures. It extends the traditional evolutionary algorithms (like Genetic Algorithms (GAs)) by incorporating a belief space that guides the evolution process. This belief space stores knowledge acquired by the population over time and influences the behavior of future generations.

Cultural algorithms are fundamentally composed of two key components: the Population Space and the aforementioned Belief Space, which are dual inheritance systems. The process starts with a randomly generated population space. Additionally, the belief space's overall structure is initialized with suitable values. The fitness functions of the individuals are then evaluated. To maintain the belief space up to date, the accept function selects a predetermined number of individuals with the lowest fitness function values from the population space. A new generation of individuals is created through the influence function.

A new group of individuals is subsequently generated by leveraging the knowledge kept in the belief space. In this phase, the impact of two different kinds of information (situational and normative) can be employed to shape the characteristics of the next generation. The direction of the search is established based on situational knowledge, and the step size is decided by the normative knowledge component. An expression of this impact function is given in equation (11):

$$x_{i,j}^{t+1} = \begin{cases} x_{i,j}^{t} + |\, size(I_j^t) N_{i,j}(0,1) \,| \; if \; x_{i,j}^{t} < s_j^t \\ x_{i,j}^{t} - |\, size(I_j^t) N_{i,j}(0,1) \,| \; if \; x_{i,j}^{t} > s_j^t \\ x_{i,j}^{t} + size(I_j^t) N_{i,j}(0,1) \quad otherwise \end{cases} \tag{11}$$

The primary steps of the CA algorithm are described in detail in (Maheri et al., 2021).

3.3 Invasive Weed Optimization (IWO)

The population-based meta-heuristic optimization approach known as IWO draws inspiration from nature, being modeled on the colonizing behavior of invasive weeds. It was suggested by Mehrabian & Lucas (2006) and is particularly known for its simplicity, robustness, and strong global search capability. Invasive weeds spread rapidly and adapt to various environmental conditions, they grow, reproduce, and dominate an ecosystem due to their strong reproductive ability and natural selection. This method is straightforward yet efficient in identifying the best solutions in a weed colony by using simple characteristics like spawning, growth, and competition (Misaghi & Yaghoobi, 2019).

Each seed develops into a blossoming plant that then yields more seeds based on its fitness value. The quantity of plant seeds drops linearly from S_{max} to S_{min}, as expressed by equation (12):

$$S_i = \left(S_{\min} + \frac{S_{\max} - S_{\min}}{f_{\min} - f_{\max}} \times \left(f\left(X_j\right) - f_{\max} \right) \right), \quad j = 1, 2, \ldots, M \tag{12}$$

with X_j being the j-th solution.

Equation (13) provides the standard deviation (SD), average planting site, and number of seeds produced by the normal distribution group:

$$\sigma^t = \frac{(T-t)^\beta}{T^\beta}\left(\sigma_{initial} - \sigma_{final}\right) + \sigma_{final} \tag{13}$$

The initial and final standard deviations are denoted by $\sigma_{initial}$ and σ_{final}, respectively, where σ^t is the standard deviation for the current iteration t, and T is the maximum number of iterations. β denotes a nonlinear modulus, also known as a nonlinear modulation index.

The following new solutions are generated once the standard division is evaluated:

$$X_r^{(new)} = Mrand\left(0, \sigma_t\right) + X_j \text{ , with } j = 1, 2, \ldots M, \; r = 1, 2, \ldots S_i \tag{14}$$

Misaghi & Yaghoobi (2019) provide a detailed description of the IWO algorithm's main phases.

3.4 Black Hole Algorithm (BHA)

The Black Hole Algorithm is a population-based meta-heuristic optimization technique, drawing inspiration from astrophysics. It was proposed by Hatamlou (2013), and it uses the gravitational pull of a black hole as a metaphor for guiding candidate solutions toward optimality. In the proposed BHA, a population of candidate solutions (stars) is explored within a n-dimensional search space to identify the optimal solutions, where there are upper and lower limits for each dimension. At each iteration t, the best solution (with the lowest or highest fitness depending on the problem) becomes the black hole x_{BH}.

The black hole being found, once the stars are put into motion, it starts to devour the neighboring stars. Consequently, every star is attracted to the black hole, and its formula for star absorption is as follows:

$$x_i(t+1) = x_i(t) + rand \times \left(x_{BH} - x_i(t)\right), \quad i = 1, 2, \ldots, N \tag{15}$$

where rand is an arbitrary integer between *0* and *1* and $x_i(t+1)$ and $x_i(t)$ represent the i-th star's positions at iterations $t+1$ and t, respectively. The search area at x_{BH} includes the black hole. Notably, the black hole remains stationary as it possesses the highest fitness value, thereby attracting all other stars. Here, N represents the total number of candidate solutions. If a star is at a distance lower than the Schwarzschild radius from the black hole, it dies. A new star must emerge and be distributed at random over the search area to maintain a consistent number of solutions or candidate stars; the BHA determines the radius of the event horizon using equation (16):

$$R = \frac{f_{BH}}{\sum_{N}^{i=1} f_i} \tag{16}$$

Hatamlou (2013) provides a thorough explanation of the key stages of the BHA algorithm.

4. Birotor Coaxial UAV Control

Initially, the inputs to the simulation system must be defined in terms of lift and drag coefficients, inclinations, and motor rotation speeds. This is accomplished using the birotor coaxial UAV's dynamics equations (1) to (6) as a basis:

$$\begin{cases} C_1 = \frac{1}{2}\rho S 0.1(1+\alpha) R^2 \left(\Omega_{hi}^2 + \Omega_{hs}^2\right) \\ C_2 = \frac{1}{2}\rho S 0.1(1+\beta) R^2 \left(\Omega_{hi}^2 + \Omega_{hs}^2\right) \\ U_1 = (b_s + b_i)\left(\Omega_{hi}^2 + \Omega_{hs}^2\right) \\ U_2 = d_{hs}\left(\Omega_{hs}^2 - \Omega_{hi}^2\right) \end{cases} \tag{17}$$

4.1 Control Design

The current study implemented PD controllers to achieve the effective control of the aircraft system. Accordingly, the nonlinear birotor model is regulated using six PD controllers, with the transfer functions taking the form $C_i(p)^{PD}$ with $i = \{\phi,\theta,\psi,x,y,z\}$:

$$C_i(p)^{PD} = K_{pi} + K_{di}\,p \tag{18}$$

The command entries linked to ϕ, θ, and ψ are denoted as C_1, C_2, and U_4, respectively. Additionally, the variables ϕ, θ, and U_1 are used for generating two virtual commands that allow the independent control of each output. Equation (19) defines these virtual commands. At the level of the UAV body, this means that the translational movement related to the axes x, y and z is indirectly controlled by the common inputs φ, θ and U_1:

$$\begin{bmatrix} U_x \\ U_y \end{bmatrix} = \begin{bmatrix} \frac{U_1}{m}\left(\cos(\phi)\sin(\theta)\cos(\psi)+\sin(\phi)\sin(\psi)\right) \\ \frac{U_1}{m}\left(\cos(\phi)\sin(\theta)\sin(\psi)-\sin(\phi)\cos(\psi)\right) \end{bmatrix} \tag{19}$$

While the PD law of command executes the virtual U_i command where $i=\{x, y\}$, the desired roll φ_d and pitching θ_d rotations are obtained from equation (19) in order to respect the desired trajectories of x and y:

$$\begin{cases} \phi_d = \arcsin\left(\frac{m}{U_1}\left(U_x\sin(\psi_d)-U_y\cos(\psi_d)\right)\right) \\ \theta_d = \arcsin\left(\frac{m}{U_1\cos(\phi_d)}\left(U_x\cos(\psi_d)+U_y\sin(\psi_d)\right)\right) \end{cases} \tag{20}$$

Figure 2 depicts the birotor's control system, where PD controllers stabilize the attitudes (ϕ, θ, ψ) and altitude (z), while two additional PD controllers regulate the x and y positions.

4.2 Meta-heuristic Algorithms Based Control

CA, BHA, ACO, and IWO are advanced intelligent techniques well-suited for handling nonlinear systems. The nonlinear and fully coupled dynamics of the birotor, described by equations (8)-(13), can be directly regulated through these approaches, where the algorithms are employed to optimize the PD controller parameters across all the six outputs. For a fair benchmarking, the initial populations of ACO, CA, IWO and BHA are randomly distributed within a search space of dimension D=12, and the number of iterations is kept identical for all the methods (20 iterations).

The objective function given in equation (22) is the step response characteristic, which comprises the maximum overshoot O_v, the settling time T_s, and the Integral of Time-weighted Absolute Error (ITAE) in equation (21), where the weighting factors w_1, w_2, and w_3 have the values 0.2, 0.1 and 0.7, respectively:

$$ITAE = \int_0^{\infty} t\,|\,e(t)\,|\,dt \tag{21}$$

$$f = w_1(\sum O_{vi}) + w_2(\sum T_{si}) + w_3\sum ITAE_j \quad j=\{x,y,z,\phi,\theta,\psi\}\ ;\ i=\{x,y,z\} \tag{22}$$

The weighting coefficients of the objective function were obtained through a preliminary optimization study rather than being chosen arbitrarily. Different weight combinations were evaluated for identifying the best compromise between tracking accuracy, transient response, and robustness, with the higher weights explicitly prioritizing the corresponding sub-fitness terms. The selected weights yield the lowest overall fitness value, as confirmed by the sensitivity analysis shown in Figure 3.

The performance of the considered meta-heuristic algorithms was assessed based on four evaluation metrics: Standard deviation (SD), Average cost, Worst cost and Best cost.

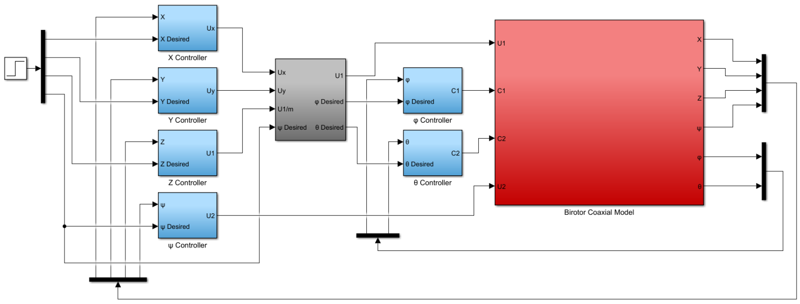

Figure 2. Coaxial Birotor UAV control loop

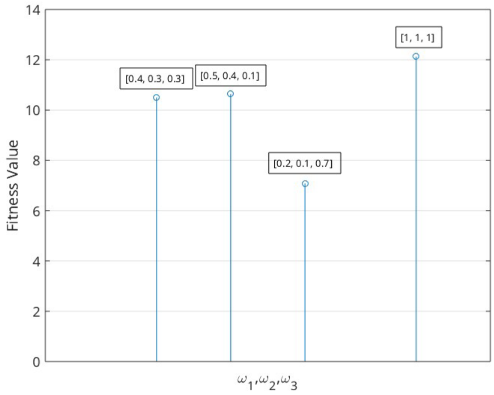

Figure 3. Weighting Coefficient Selection

5. Results and Discussion

The intelligent PD controllers are applied to the birotor's position (x,y,z) and attitude (ϕ,θ,ψ). Their performance with CA, IWO, ACO and BHA is tested in hovering and trajectory-tracking scenarios, showing an effective path following even under disturbances. The parameters of the coaxial birotor UAV are listed in Table 1, the proposed dynamic trajectories are expressed in equation (23) and equation (24) and Table 2 shows the PD parameters for the coaxial birotor UAV outputs obtained by using ACO, CA, IWO and BHA algorithms.

Table 1. The parameters of the coaxial birotor UAV

Parameters	Values
$m\,(kg)$	0.6
$g\,(m/s^2)$	9.806
$L_d(m)$	0.17
C_T	0.115
C_s, C_i	0.07
$d_{hs}, d_{hi}(N\cdot m.s^2)$	3×10^{-6}
$I_x(kg\cdot m^2)$	5.12×10^{-4}
$I_y(kg\cdot m^2)$	5.3×10^{-4}
$I_z(kg\cdot m^2)$	8.16×10^{-4}

• First trajectory

$$\begin{cases} x_d = 1(m) \\ y_d = 1(m) \\ z_d = 1(m) \\ \psi_d = 1(rad) \end{cases} \quad (23)$$

• Second trajectory (Helicoidal)

$$\begin{cases} x_d = \sin\left(0.3t + \dfrac{\pi}{2}\right) \\ y_d = \sin(0.3t) \\ z_d = 0.1t \\ \psi_d = 0 \end{cases} \quad (24)$$

Table 2. PD parameters for the coaxial birotor UAV outputs obtained by using ACO, CA, IWO and BHA

PDs Gains		Algorithms			
		ACO	CA	IWO	BHA
ϕ	K_p	1.5649	0.9546	1.6889	1.026
	K_d	0.6567	0.2752	0.2966	0.5255
θ	K_p	1.1412	1.3093	1.9366	1.3021
	K_d	0.3052	0.2637	0.1298	0.6146
ψ	K_p	1.8638	1.6084	1.5803	1.6239
	K_d	1.5891	1.3755	1.7715	1.0105
x	K_p	6.74	5.3067	7.6104	3.6021
	K_d	9.89	7.2159	9.3689	6.0209
y	K_p	4.46	3.7748	6.533	2.8203
	K_d	8.94	6.2517	9.001	5.4158
z	K_p	131.43	181.58	187.55	156.81
	K_d	31.884	50.188	72.792	54.968

Figure 4 shows the rate of convergence for the employed techniques. It was shown that IWO-PD and CA-PD had the fastest rate of convergence and required the fewest iterations (less than 20) to obtain values that were near the optimal value. BHA-PD also obtained satisfactory results in

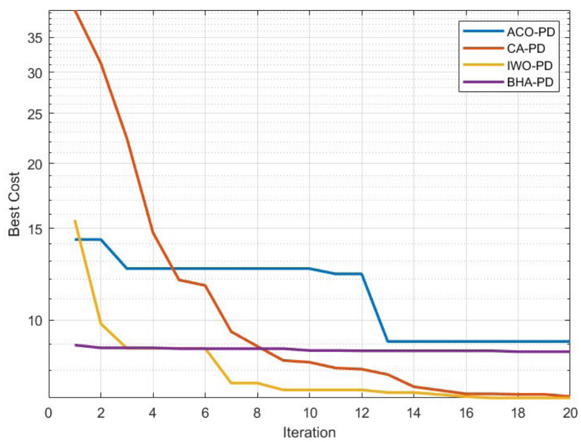

Figure 4. Convergence rate of ACO, CA, IWO and BHA

terms of achieving the optimal value, but it was unable to get past the local optima. With regard to ACO-PD, it failed to obtain the optimal solution even after more than 20 iterations.

Table 3 shows the fitness function values for five runs of the employed algorithms. The IWO (with a best value of 7.0832) with a SD of 0.3122 obtained the best values for the objective function, indicating that it is the most efficient. This behavior can be conceptually explained by the exploration–exploitation nature of IWO: its adaptive spreading mechanism allows a wide initial exploration of the solution space, followed by a gradual concentration around the promising regions. Such a strategy is particularly effective for the highly nonlinear and coupled dynamics of a birotor UAV, where multiple local minima exist in the controller parameter space due to the interaction between roll, pitch, and vertical motion. Similarly, in (Azegmout et al., 2023) IWO provides a higher performance in terms of optimizing the PID parameters for various system behaviors with the fastest CPU time, indicating its superior performance in the context of the PID parameter problem. In contrast, while ACO is effective for handling discrete problems, when applied to large-scale datasets it is inherently constrained by a limited convergence speed and a reduced solution accuracy (Yu et al., 2021).

Table 3. Values of the fitness function for 5 runs of the employed meta-heuristic algorithms (significant values are rendered in bold)

Number of runs	Algorithms			
	ACO	CA	IWO	BHA
1	9.8004	9.0883	7.2705	9.5560
2	9.4688	7.1281	7.8985	8.9850
3	9.4257	8.9045	7.2941	8.6931
4	9.1239	8.7514	7.5184	8.8804
5	9.0969	8.3123	**7.0832**	9.1878
Best	9.0969	7.1281	**7.0832**	8.6931
Worst	9.8004	9.0883	**7.8985**	9.5560
Average	9.3831	8.4369	**7.4129**	9.0605
Standard Deviation (SD)	0.2882	0.7858	**0.3122**	0.3297

5.1 Initial Trajectory Results

The outputs (x, y, z, ψ) and their step responses, obtained via ACO, CA, IWO and BHA are illustrated in Figure 5. The desired roll and pitch angles (ϕ and θ) are computed based on the selected yaw angle (ψ_desired) and the responses from the x- and y-axis controllers, therefore their desired values will differ; the required and regulated roll (ϕ) and pitch (θ) angle responses are shown in Figure 6 and Figure 7 and the values of the ISE and ITAE errors for the initial trajectory tracking are shown in Table 4.

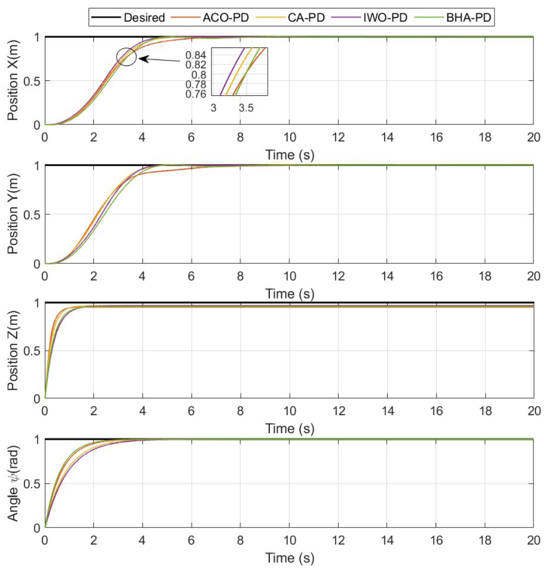

Figure 5. Desired and controlled coaxial birotor UAV position (x,y,z) and yaw angle (ψ) by using ACO, CA, IWO and BHA

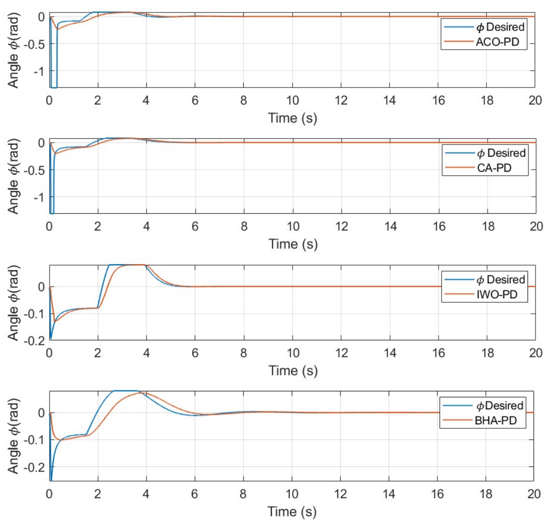

Figure 6. Desired and controlled roll angle (ϕ) by using ACO, CA, IWO and BHA

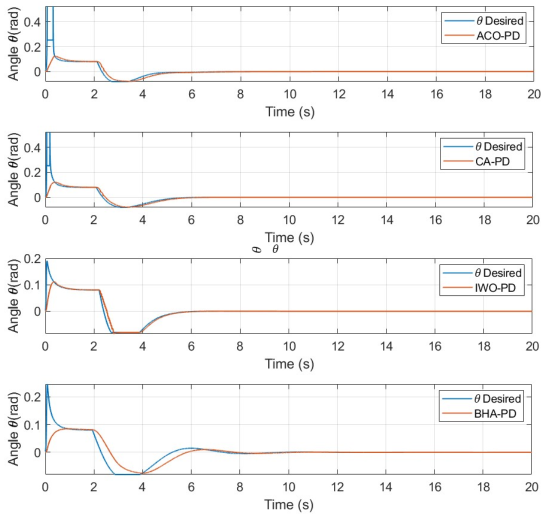

Figure 7. Desired and controlled pitch angle (θ) by using ACO, CA, IWO and BHA

Table 4. Coaxial birotor UAV errors (ISE and ITAE) measured by using ACO, CA, IWO and BHA for the first trajectory

Outputs		Algorithms			
		ACO	**CA**	**IWO**	**BHA**
x	ISE	2.0042	1.9392	1.8837	2.0602
	ITAE	4.3110	3.6359	3.4279	4.1541
y	ISE	1.6992	1.6990	1.7991	1.9102
	ITAE	3.8761	2.9429	3.1488	3.7769
z	ISE	0.1773	0.1736	0.2304	0.2226
	ITAE	9.2240	6.7125	6.5739	7.8064
ϕ	ISE	0.3534	0.1953	0.0041	0.0097
	ITAE	0.4379	0.2698	0.1573	0.4857
θ	ISE	0.0125	0.0106	0.0030	0.0100
	ITAE	0.1844	0.1415	0.0787	0.4820
ψ	ISE	0.4291	0.4309	0.5630	0.3157
	ITAE	0.7221	0.7257	1.2509	0.3815

5.2 Helicoidal Trajectory Results

The outcomes of the proposed method are also displayed for a helicoidal trajectory scenario, in contrast to the first route that entails lingering at predetermined coordinates. In this sense, Figure 8 depicts the tracking of the desired path for each positional coordinate (x, y, z), while Figures 9 and 10 display the desired and regulated roll (ϕ) and pitch (θ) angle responses; it is evident that the four employed meta-heuristic algorithms accurately interpret the information from the sensors. Furthermore, Table 5 demonstrates that for various outputs of the coaxial birotor UAV, IWO obtained the lowest ISE and ITAE errors.

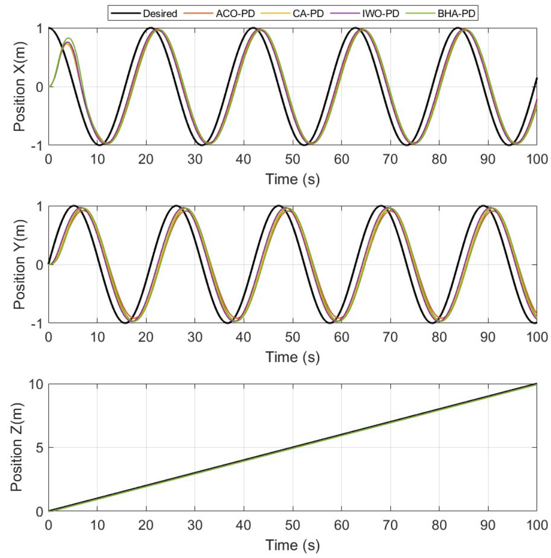

Figure 8. Desired and controlled coaxial birotor UAV position (x,y,z) by using ACO, CA, IWO and BHA

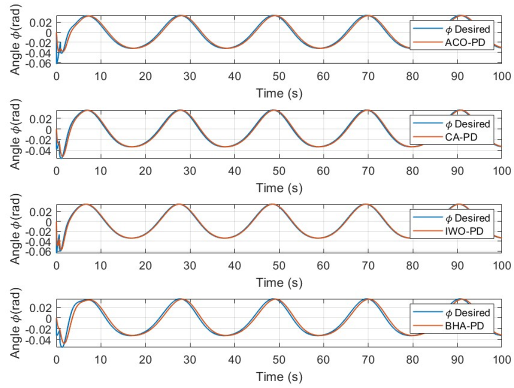

Figure 9. Desired and controlled roll angle (ϕ) by using ACO, CA, IWO and BHA

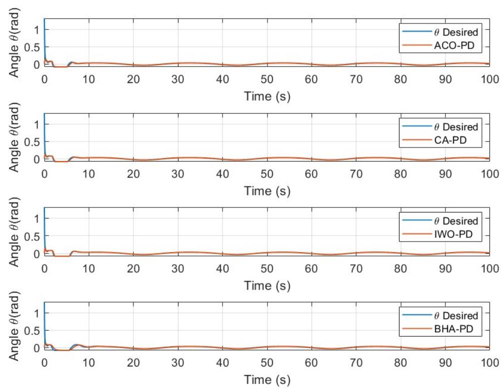

Figure 10. Desired and controlled pitch angle (θ) by using ACO, CA, IWO and BHA

Figure 11 displays the tracking of both the controlled and planned flight trajectories within a three-dimensional spatial framework.

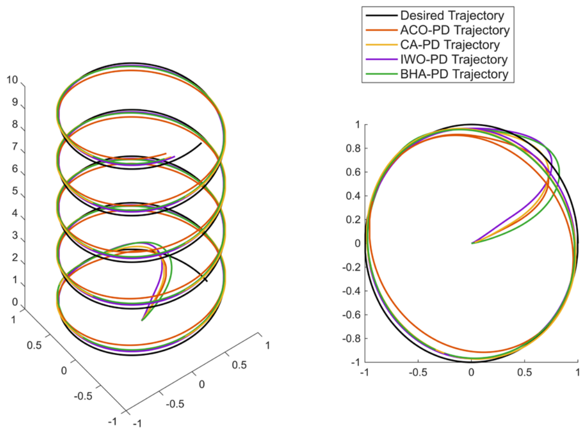

Figure 11. Desired and controlled coaxial birotor UAV trajectories by using ACO, CA, IWO and BHA in 3D (helicoidal trajectory)

These findings unequivocally demonstrate the proposed system's ability to precisely track the coaxial birotor UAV's trajectories for all variables (yaw angle, the translation motion related to the x and y axes, and altitude z).

Table 5. Birotor errors (ISE and ITAE) measured by using ACO, CA, IWO and BHA for the second trajectory

Outputs		Algorithms			
		ACO	CA	IWO	BHA
x	ISE	10.241	9.5849	8.3238	13.409
	ITAE	1.3320e+03	1.2754e+03	1.1540e+03	1.5327e+03
y	ISE	14.517	11.405	7.9031	14.766
	ITAE	1.7528e+03	1.5415e+03	1.2818e+03	1.7571e+03
z	ISE	0.4909	0.3690	0.5010	0.5380
	ITAE	350.71	304.25	354.83	367.56
ϕ	ISE	0.0016	8.5258e-04	4.8312e-04	0.0024
	ITAE	13.248	9.6381	5.8401	17.078
θ	ISE	0.0904	0.0664	0.0620	0.0842
	ITAE	8.6449	6.6476	2.2710	15.767
ψ	ISE	0	0	0	0
	ITAE	0	0	0	0

5.3 Helicoidal Trajectory Results in the Presence of Disturbances

Wind disturbances along the z-axis represent the most significant external forces acting on the coaxial birotor UAV and they are modeled as a variable-amplitude disturbance applied to a closed-loop system for testing the robustness of CA, ACO, BHA, and IWO controllers. As shown in Figures 12–15, all four controllers produce responses closely matching the desired trajectories while effectively mitigating the disturbance effects. Minor deviations are observed for the X and Y positions from the initial sinusoidal paths, likely to maintain the altitude (z) close to its intended trajectory.

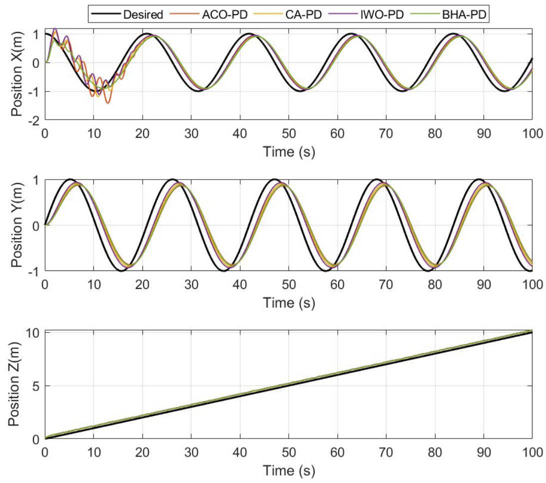

Figure 12. Desired and controlled coaxial birotor UAV position (x,y,z) by using ACO, CA, IWO and BHA in the presence of external disturbances

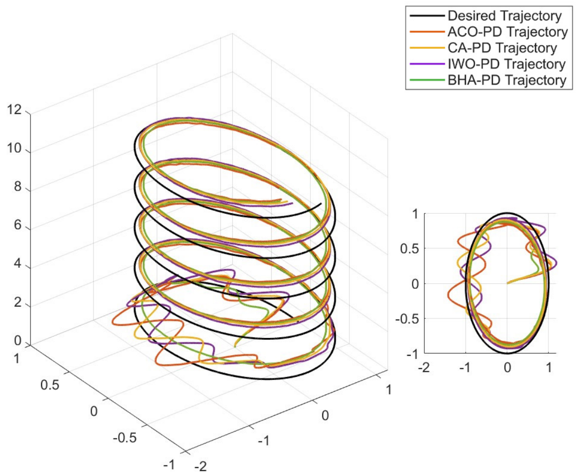

Figure 13. Desired and controlled coaxial birotor UAV trajectories by using ACO, CA, IWO and BHA in the presence of external disturbances in 3D

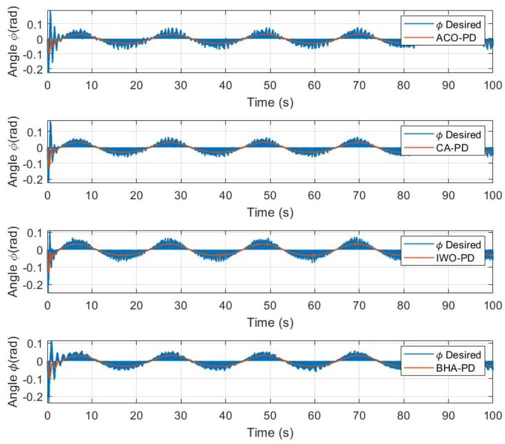

Figure 14. Desired and controlled roll angle (ϕ) by using ACO, CA, IWO BHA in the presence of external disturbances and

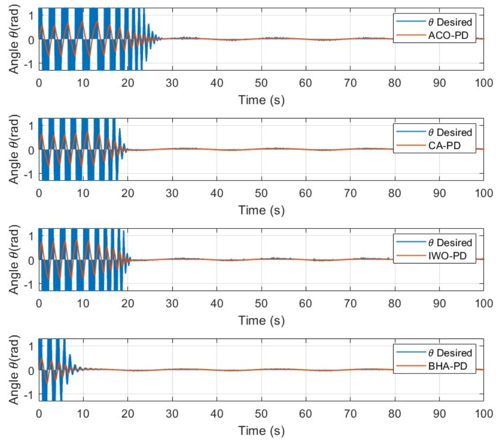

Figure 15. Desired and controlled pitch angle (θ) by using ACO, CA, IWO and BHA in the presence of external disturbances

Table 6 summarizes the performance of ACO, CA, IWO and BHA with regard to the birotor's outputs (ϕ, θ, ψ, x, y, z) during hovering flight, evaluated by using the fitness function in equation (22). The obtained results demonstrate that the proposed controllers ensure a precise regulation of the birotor's dynamics, effectively minimizing the overshoot, the mean squared error and settling time. For benchmarking purposes, these results are compared with those obtained by using other approaches such as the PSO-optimized PD controller developed for a tandem tilt-rotor UAV (El Gmili et al., 2019a) as well as the GS-NNPD (El Hamidi et al. 2022) and PSO-CS-PID (El Gmili et al., 2019b) controllers. El Hamidi et al. (2022) introduced two adaptive control strategies for quadcopter path tracking: a Gain-Scheduling Neural Network-based PID/PD controller (GS-NN-PID/PD) and a Fuzzy PID/PD controller optimized by using Particle Swarm Optimization (FPID/PD-PSO). Their results demonstrated that both approaches achieved faster responses, an improved performance, and an enhanced robustness in comparison with the classical fuzzy PID/PD controller. Further on, Particle Swarm Optimization (PSO), Cuckoo Search (CS), and a hybrid PSO-CS algorithm are used in the quadrotor UAV control strategy

Table 6. The performance achieved by ACO, CA, IWO and BHA for the birotor and comparison with other models and control methods

Performance for the coaxial birotor UAV outputs		Approaches						
		Proposed Algorithms				References		
		ACO	**CA**	**IWO**	**BHA**	**PSO-PD (El Gmili et al., 2019a)**	**GS-NNPD (El Hamidi et al., 2022)**	**PSO-CS-PID (El Gmili et al., 2019b)**
x	$T_s(s)$	5.9717	4.6893	4.4407	4.531	3.4503	0.94	0.522
	$O_v(\%)$	0	0.038	0.2083	0.1968	1.8e-07	0	0.446
	MSE	0.1002	0.097	0.0942	0.103	30.889	0.0333	-
y	$T_s(s)$	6.6256	4.2716	4.196	4.4173	4.1445	0.81	0.782
	$O_v(\%)$	0	0.078	0.1711	0.3427	0.0684	0	0.010
	MSE	0.085	0.085	0.09	0.0955	17.864	0.0334	-
z	$T_s(s)$	0.8611	1.0431	1.4945	1.3391	2.7608	0.64	0.813
	$O_v(\%)$	0	0	0	0	0.4836	0	0.002
	MSE	0.0089	0.0087	0.0115	0.0112	1.3477	0.0155	-
ϕ	$T_r(s)$	-	-	-	-	-	-	-
	$O_v(\%)$	-	-	-	-	-	-	-
	MSE	0.0177	0.0098	2.e-04	4.8e-04	0.0007	0.0008	-
θ	$T_s(s)$	-	-	-	-	-	-	-
	$O_v(\%)$	-	-	-	-	-	-	-
	MSE	6.2e-04	5.2e-04	1.5e-04	4.9e-04	0.0084	0.0327	-
ψ	$T_s(s)$	3.3189	3.3262	4.3705	2.4074	0.0172	0.153	0.097
	$O_v(\%)$	0	0	0	0	-	0	0.047
	MSE	0.0215	0.0216	0.0282	0.0158	1.96e-8	0.0028	-

presented in (El Gmili et al., 2019b). The obtained results demonstrate that the mixed PSO-CS algorithm outperforms the CS and PSO tuning methods, especially in trajectory tracking and disturbance rejection including the case when wind disturbances are present. It is also worth mentioning the single-rotor UAV control strategy proposed by Portillo et al. (2023), in which PID, Super-Twisting, and Adaptive Sliding Mode controllers were finely tuned by using Particle Swarm Optimization (PSO) in order to improve trajectory tracking performance and disturbance rejection. Among these, the Super-Twisting Controller (ST-PSO) exhibited a superior performance, providing smoother tracking responses and an improved resilience to modeling uncertainties.

This comparison highlights the superior control capability of the coaxial birotor UAV configuration over that of conventional UAV designs. Although the PSO-based tuning provided satisfactory outcomes for the tandem rotor UAVs, the metaheuristic-based PD controllers proposed for the coaxial birotor exhibited more stable and accurate responses. Among the tested algorithms, the IWO achieved the best performance, demonstrating its superior optimization accuracy, robustness, and computational efficiency.

In summary, these benchmarks demonstrate that combining the coaxial birotor UAV model based on the Newton–Euler formalism with metaheuristic optimization algorithms enables a superior control performance. The proposed approach provides a precise trajectory tracking and strong disturbance rejection, making the birotor UAV particularly suited for operations in indoor or confined environments, where a high stability and accuracy are required.

5.4 Limitations and Future Work

Future work could focus on the experimental validation of the proposed PD-based tuning approach for a real coaxial birotor UAV. This will involve testing the robustness of the optimized controllers under realistic disturbances, imperfections, and sensor hardware constraints. Additionally, the computational efficiency of metaheuristics in real-time applications could be investigated and adaptive or online optimization strategies for real-time PD controller adjustment could be explored.

6. Conclusion

This study proposed a complete control framework for a Coaxial Birotor UAV, starting from a Newton–Euler–based mathematical model and extending to the design of six PD controllers for translational (x,y,z) and rotational (ϕ,θ,ψ) dynamics. In order to address the limitations of conventional gain selection, four meta-heuristic algorithms, namely IWO, ACO, CA and BHA were employed for optimally tuning the PD parameters. The proposed controllers were validated through trajectory tracking simulations using two scenario paths, and their robustness was tested under external disturbances.

The obtained results showed that metaheuristic-based tuning significantly enhanced the UAV trajectory tracking performance, reducing the overshoot, settling time, and tracking error in comparison with the classical methods. Among the tested algorithms, IWO consistently outperformed ACO, CA and BHA, achieving the best cost value of 7.0832 with the lowest variance. These outcomes confirm IWO's superior balance between optimization accuracy, robustness, and computational efficiency in tuning PD controllers for a nonlinear UAV dynamics.

Overall, the findings highlight the effectiveness of metaheuristic optimization for UAV control, offering a precise trajectory tracking and strong disturbance rejection. Future work will also focus on development of hybrid optimization strategies that combine the strengths of different metaheuristics, aiming to further improve convergence speed, robustness, and scalability for more complex UAV configurations.

REFERENCES

Ait Dahmad, H., Ayad, H., García Cerezo, A. et al. (2025) Adaptive Model Predictive Control for 4WD-4WS Mobile Robot: A Multivariate Gaussian Mixture Model-Ant Colony Optimization for Robust Trajectory Tracking and Obstacle Avoidance. *Sensors*. 25(12), 3805. https://doi.org/10.3390/s25123805.

Alaimo, A., Artale, V., Milazzo, C. L. R. et al. (2014) PID Controller Applied to Hexacopter Flight. *Journal of Intelligent & Robotic Systems*. 73, 261–270. https://doi.org/10.1007/s10846-013-9947-y.

Azegmout, M., Mjahed, M., El Kari, A. et al. (2023) New Meta-heuristic-Based Approach for Identification and Control of Stable and Unstable Systems. *International Journal of Computers, Communications & Control*. 18(4), Art. ID 5294. https://doi.org/10.15837/ijccc.2023.4.5294.

Azegmout, M., Mjahed, M., El Kari, A. et al. (2024) Birotor Coaxial Model Estimation using Different Influence Function of Cultural Algorithm. In: *International Conference on Mobility, Artificial Intelligence and Health (MAIH2024)* (*ITM Web of Conferences*, *vol. 69), 20-22 November 2024, Marrakech, Morocco*. Les Ulis, France, EDP Sciences. https://doi.org/10.1051/itmconf/20246901012.

Bermes, C. (2010). *Design and dynamic modeling of autonomous coaxial micro helicopters.* PhD thesis, ETH Zurich, Switzerland.

Darvishpoor, S., Roshanian, J., & Tayefi, M. (2015) A novel concept of VTOL bi-rotor UAV based on moving mass control. *Aerospace Science and Technology*. 107, Art. ID 106238. https://doi.org/10.1016/j.ast.2020.106238.

Donadel, R., Raffo, G. V. & Becker, L. B. (2014) Modeling and Control of a Tiltrotor UAV for Path Tracking. *IFAC Proceedings Volumes*. 47(3), 3839–3844. https://doi.org/10.3182/20140824-6-ZA-1003.01735.

Dorigo, M. (1992) *Optimization, Learning and Natural Algorithms.* PhD thesis, Polytechnic University of Milan.

Driessens, S. & Pounds, P. (2015) The Triangular Quadrotor: A More Efficient Quadrotor Configuration. *Automation in Construction*. 31(6), 1517–1526. https://doi.org/10.1109/TRO.2015.2479877.

El Gmili, N., Mjahed, M., El Kari, A. et al. (2019a) Particle swarm optimization based proportional-derivative parameters for unmanned tilt-rotor flight control and trajectory tracking. *Automatika*. 61(2), 189–206. https://doi.org/10.1080/00051144.2019.1698191.

El Gmili, N., Mjahed, M., El Kari, A. et al. (2019b) Particle Swarm Optimization and Cuckoo Search-Based Approaches for Quadrotor Control and Trajectory Tracking. *Applied Sciences*. 9(8), 1719. https://doi.org/10.3390/app9081719.

El Hamidi, K., Mjahed, M., El Kari, A. et al. (2022) Neural Network and Fuzzy-logic-based Self-tuning PID Control for Quadcopter Path Tracking. *Studies in Informatics and Control.* 28(4), 401–412. https://doi.org/10.24846/v28i4y201904.

Ezzara, A., Ouadine, A, Y. & Ayad, H. (2025) Adaptive Backstepping Active Fault-Tolerant Control with Nonlinear Adaptive Observer for Quadrotor UAV Under Actuator Faults and Disturbances. *Studies in Informatics and Control*. 34(1), 85-95. https://doi.org/10.24846/v34i1y202507.

Fayti, M., Mjahed, M., Ayad, H. et al. (2023) Recent Metaheuristic-Based Optimization for System Modeling and PID Controllers Tuning. *Studies in Informatics and Control.* 32(1), 57–67. https://doi.org/10.24846/v32i1y202306.

Hatamlou, A. (2013) Black hole: A new heuristic optimization approach for data clustering. *Information Sciences*. 222, 175–184. https://doi.org/10.1016/j.ins.2012.08.023.

Koehl, A., Rafaralahy, H., Boutayeb, M. et al. (2012) Aerodynamic Modelling and Experimental Identification of a Coaxial-Rotor UAV. *Journal of Intelligent & Robotic Systems*. 68, 53–68. https://doi.org/10.1007/s10846-012-9665-x.

Maheri, A., Jalili, S., Hosseinzadeh, Y. et al. (2021) A comprehensive survey on cultural algorithms. *Swarm and Evolutionary Computation*. 62, Art. ID 100846. https://doi.org/10.1016/j.swevo.2021.100846.

Mehrabian, A. R. & Lucas, C. (2006) A novel numerical optimization algorithm inspired from weed colonization. *Ecological Informatics*. 1(4), 355–366. https://doi.org/10.1016/j.ecoinf.2006.07.003.

Misaghi, M. & Yaghoobi, M. (2019) Improved invasive weed optimization algorithm (IWO) based on chaos theory for optimal design of PID controller. *Journal of Computational Design and Engineering.* 6(3), 284–295. https://doi.org/10.1016/j.jcde.2019.01.001.

Mjahed, M. & Said, F. (2018) *Design and Implementation of a Birotor Coaxial UAV*. Graduation Project, Royal School of Aeronautics, Marrakech, Morocco.

Mjahed, M. (2019). Flight control system design using neural networks. *International Robotics & Automation*

Journal. 5(3), 96–98. https://doi.org/10.15406/iratj.2019.05.00180.

Niu, S., Li, J. & Shen, Y. (2015) Design, modeling and disturbance rejection control of a bio-inspired coaxial helicopter MAV in atmospheric boundary layer. In: 2015 *IEEE International Conference on Robotics and Biomimetics (ROBIO), 6-9 December 2015, Zhuhai, China*. New York, USA, IEEE. pp. 1272–1277.

Nkouagnou, C. J., Haman, D. & Kenfack, J. A. (2021) Trajectory Tracking Controller for Birotor Coaxial UAV Using Nonlinear Continuous-Time Generalized Predictive Control Combined with a PI-Observer. *Russian Aeronautics*. 64, 646–660. https://doi.org/10.3103/S1068799821040097.

Nonami, K., Kendoul, F., Suzuki, S. et al. (2010) *Autonomous Flying Robots: Unmanned Aerial Vehicles and Micro Aerial Vehicles*. Springer.

Portillo, P., Garza-Castañón, L. E., Minchala-Avila, L. I. et al. (2023) Robust Nonlinear Trajectory Controllers for a Single-Rotor UAV with Particle Swarm Optimization Tuning. *Machines*. 11(9), 870. https://doi.org/10.3390/machines11090870.

Pounds, P. E. I., Bersak, D. R. & Dollar, A. M. (2012) Stability of small-scale UAV helicopters and quadrotors with added payload mass under PID control. *Autonomous Robots*. 33, 129–142. https://doi.org/10.1007/s10514-012-9280-5.

Qin, X. (2025) Design of Intelligent Driving Control Model Combining BP-PID and Deep Attention Mechanism. *Studies in Informatics and Control*. 34(4), 99-110. https://doi.org/10.24846/v34i4y202509.

Rakha, T. & Gorodetsky, A. (2018). Review of Unmanned Aerial System (UAS) applications in the built environment: Towards automated building inspection procedures using drones. *Automation in Construction*. 93, 252–264. https://doi.org/10.1016/j.autcon.2018.05.002.

Reynolds, R. (1994) An introduction to cultural algorithms. In: *Proceedings of the Third Annual Conference on Evolutionary Programming*, *24-26 February 1994, San Diego, USA*. pp. 131–139.

Roussel, E., Gassmann, V. & Laroche, E. (2016) Modelling and identification of a coaxial birotor UAV from scarce flight data. In: *2016 European Control Conference (ECC), 29 June - 1 July 2016, Aalborg, Denmark.* New York, USA, IEEE. pp. 2158–2164.

Siti, I., Mjahed, M., Ayad, H. et al. (2019) New Trajectory Tracking Approach for a Quadcopter Using Genetic Algorithm and Reference Model Methods. *Applied Sciences*. 9(9), 1780. https://doi.org/10.3390/app9091780.

Ünal, M., Ak, A., Topuz, V. et al. (2013) *Optimization of PID Controllers Using Ant Colony and Genetic Algorithms*. Berlin, Heidelberg, Springer.

Varol, H. A. & Bingul, Z. (2004) A new PID tuning technique using ant algorithm. In: *Proceedings of the 2004 American Control Conference*, *30 June - 2 July 2004, Boston, USA*. New York, USA, IEEE. pp. 2154–2159.

Wang, X., Li, K., Zhao, N. et al. (2017) Nonlinear dynamics modeling and simulation of cylindrical coaxial UAV. In: *IEEE International Conference on Real-time Computing and Robotics (RCAR), 14-18 July 2017, Okinawa, Japan*. New York, USA, IEEE. pp. 505–510.

Xu, J., Hao, Y., Wang, J. et al. (2021) The Control Algorithm and Experimentation of Coaxial Rotor Aircraft Trajectory Tracking Based on Backstepping Sliding Mode. *Aerospace.* 8(11), 337. https://doi.org/10.3390/aerospace8110337.

Xu, A., Wang, F. & Chen, M. (2022) Modeling and Robust Tracking Decoupling Control of a Coaxial Unmanned Helicopter Based on the Improved Alternating Direction Method of Multipliers. *Computational Intelligence and Neuroscience*. Art. ID 3647784. https://doi.org/10.1155/2022/3647784**.**

Yu, J., You, X. & Liu, S. (2021) A heterogeneous guided ant colony algorithm based on space explosion and long–short memory. *Applied Soft Computing*. 113(B), Art. ID 107991. https://doi.org/10.1016/j.asoc.2021.107991.